International Journal of Thermal Sciences 48 (2009) 2221–2227

Contents lists available at ScienceDirect

International Journal of Thermal Sciences

journal homepage: www.elsevier.com/locate/ijts

Interfacial thermal resistance measurement between metallic wire and polymer in polymer matrix composites

E. Chapelle*, B. Garnier, B. Bourouga

Laboratoire de Thermocinétique, UMR CNRS 6607, Ecole Polytechnique de l'Université de Nantes, 3 rue Christian Pauc, 44300 Nantes, France

ARTICLE INFO

Article history:
Received 12 December 2008
Received in revised form
4 May 2009
Accepted 5 May 2009
Available online 14 August 2009

Keywords:
Polymer matrix composites (PMCs)
Interface
Thermal properties
Interfacial thermal resistance
Thermo-elasticity

ABSTRACT

The addition of thermally conductive particles is an effective way to increase thermal conductivity of polymers. For highly filled composites and therefore for a high effective thermal conductivity, the heat transfer at the matrix/particle interface becomes a key point to obtain further improvement. However the interfacial thermal resistance R_i between particles and matrix is difficult to measure because of the low sensitivity of temperature to R_i and because of the small size of the particles. A setup has been developed to measure R_i between nickel wires (fiber-like particles) of a few tens micrometer diameter and a polymer matrix. The temperature measurement of the heating wire associated with a thermal model allowed to estimate values of R_i between 0.3×10^{-5} and 1.6×10^{-5} $m^2\,K\,W^{-1}$ and for various wire diameters and sample temperatures. Some R_i measurements have been validated using a thermo-elastic model.

1. Introduction

The effective thermal conductivity of filled and heat-conductive polymers depends on many factors such as properties of both phases, microstructure of materials, manufacturing conditions and also on heat transfers at the particle/matrix interface. The influence of the interface is even more important if the conductivity of the composite is high, that is for large amount of particles [1]. In composites, the thermal interface resistance, R_i, may come from disparity in the physical properties of the two materials (Kapitza resistance). Surface roughness, interfacial gas and then thermal macro and microconstriction are another source of interfacial resistances. In polymer matrix composites filled with metallic particles, heat transfer at the interface can also be reduced due to thermal expansion mismatch and low adhesion between phases. In the literature, there are very few works on the determination of the interfacial thermal resistance between particle and matrix [2,3,4], partly because of the difficulties of such measurement related to the small size of the particles (from tens to a few hundred micrometers). In composites, the few R_i measurements are mainly deduced from effective thermal conductivity, knowing the composite microstructure and phase properties [2,3]. An alternative to this procedure could be the local measurement of R_i, but current progresses in thermal microscopes (SthM, AFM with thermal probe, …) fail to obtain such measurement mainly because of the presence of parasite contact resistance between probe and sample.

This work is focused on the characterization of the interfacial thermal resistance between metallic wires (fiber-like particles) and a polymer matrix. The technique used is derived from the hot-wire method [5,6] associated with a parameter estimation procedure. The second objective of this work is to study the effect of the wire diameter and of the temperature on the R_i values. Indeed, roughness of stretched metallic wires depends on the wire diameter. This should be also the case for metallic fibers in composites since they are also manufactured through die or obtained using wire cutting. In addition, temperature effect on R_i values is also studied since thermal expansion mismatch can produce unsticking at the metal/polymer interface during composite heating.

The context of this work is the improvement of effective thermal conductivity of filled polymer. The ability to perform R_i measurement would allow to study the direct effect of surface treatment (plasma, coating, …) or polymer additive (surfactant, …) on the heat transfer at the particle/matrix interface. These effects are until now observed through effective conductivity measurement ignoring the mechanisms since some of the previous treatments could change not only the matrix/particle adhesion but also the

* Corresponding author. Tel.: +33 2 40 68 31 59; fax: +33 2 40 68 31 41.
E-mail address: eric.chapelle@univ-nantes.fr (E. Chapelle).
URL: http://www.polytech.univ-nantes.fr/ltn

1290-0729/$ – see front matter © 2009 Elsevier Masson SAS. All rights reserved.
doi:10.1016/j.ijthermalsci.2009.05.001

Nomenclature

C_p	specific heat capacity, J kg^{-1} K^{-1}
dt	time interval, s
e	thickness of the nickel/epoxy gap, m
I_j, K_j	Bessel functions of order j
J	sum of the ordinary squared differences
k	thermal conductivity, W m^{-1} K^{-1}
l	mean free path, m
L	wire length, m
m	thermo-physical parameter
$\overline{M}$	air molar mass, 28.8×10^{-3} kg mol^{-1}
n	time step subscript
N	maximum number of time intervals
p	Laplace parameter
P	pressure, Pa
P_0	electrical power, W
$\overline{R}$	ideal gas constant, 8.31447 J K^{-1} mol^{-1}
R_{air}	air layer thermal resistance, m^2 K W^{-1}
R_i	interfacial thermal resistance, m^2 K W^{-1}
S	variance matrix
t	time, s
T	average temperature, °C
u	displacement, m
U	supply voltage, V
V	unbalanced voltage, V
W	variance–covariance matrix
X	sensitivity matrix
X_m	reduced sensitivity coefficient
Z	complex impedance, K W^{-1}

Greek symbols

α	thermal diffusivity, m^2 s^{-1}
β	thermal expansion coefficient, K^{-1}
δ	residual, °C
Δ	period (for time), rise (for temperature)
ε	relative error, %
θ	temperature in Laplace domain, °C
ν	Poisson's ratio
ρ	density, kg m^{-3}
σ	standard deviation
ϕ	wire diameter, m

Subscripts

ep	epoxy resin matrix
exp	experimental (for temperature)
g	gas
j	material subscript (ep or Ni)
Ni	nickel wire
RMS	root mean square

Superscript

0	free

distribution of the filler inside the composite. Enhanced effective conductivity can come also from a better design of the composite using models predicting the effective thermal conductivity. In these thermal models, it is usually supposed that the interfacial thermal resistance between particles and matrix doesn't depend on the particle size and on the temperature, this resulting mainly from the lack of R_i values.

2. Principle of the measurement method

Thermal contact resistance measurements are usually performed using plane geometry, the contact pressure being adjustable. For fibers in polymer, the contact pressure at the fiber polymer interface depends on thermal expansion mismatch, mechanical properties, processing and use temperatures, and shrinkage of polymer during polymerization. So, it is not possible to measure the contact pressure mainly because of the size of fiber or to predict it because of the complexity of the phenomena. A cylindrical geometry with a heated wire was used in order to keep the same interfacial conditions (contact pressure and also roughness) as for fibers in polymer, processing and use temperatures being controlled. This study considered fibers produced by cutting wires which is one of the cheapest ways to produce fibers.

Several cylindrical samples with metallic wires embedded in polymer were manufactured. To carry out R_i measurements between metallic wires and polymer, each metallic wire is installed as one branch of a Wheatstone bridge, and a voltage pulse provides its heating by Joule effect. The average temperature T of the wire and the electrical power are obtained from two voltage measurements: the unbalanced voltage V and the supplying voltage U of the Wheatstone bridge (Fig. 1). The temperature calibration, i.e. the relationship between T and V/U, is provided by powering the circuit with a low supplying U voltage and by varying the temperature of the sample using a temperature controlled enclosure.

Using a thermal model that describes heat transfers in the samples, the interfacial resistance R_i between metallic wire and the polymer is finally estimated from the temperature and electrical power measurements.

3. Thermal model

The thermal model has to provide the average temperature of the wire (i.e. average temperature taken all over the length of the wire) taking into account the imperfect contact, the properties and geometries of both mediums. The metallic wires are of nickel with diameters ϕ_{Ni} of 26.9, 55.8 and 122.9 μm and lengths L respectively of 25, 50 and 161 mm. As the length to diameter ratio is in the order of 1000, the heat transfer can be assumed to be 1D; 2D effects will be quantified in Section 6. For the polymer (epoxy resin), a semi-infinite boundary condition is considered since the heating time is about 10 ms. This leads to a thermal diffusion length of about 40 μm

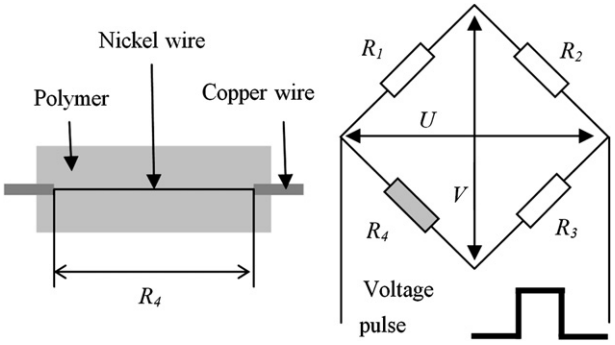

Fig. 1. Principle of the interfacial thermal resistance measurement between nickel wire and polymer matrix.

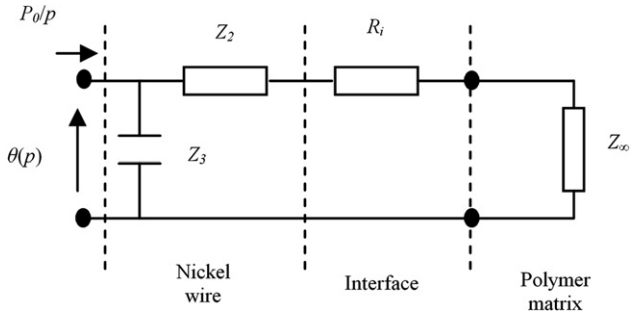

Fig. 2. Impedance network.

in the polymer, which is far lower than the sample external radius (about 8 mm).

The whole system can be represented by the impedance network shown in Fig. 2. Using the quadrupoles method [7], the average temperature θ of the metallic wire can be written in the Laplace domain as

$$\theta(p,R_i) = \frac{P_0}{p}\frac{1}{(1/Z_3)+(1/(Z_2+(R_i/\pi\phi_{Ni}L)+Z_\infty))} \quad (1)$$

$$Z_3 = \frac{4}{\rho_{Ni}C_{p_{Ni}}\pi\phi_{Ni}^2 Lp} \quad (2)$$

$$Z_2 = \frac{I_0(s)}{2\pi k_{Ni}LsI_1(s)} - Z_3 \quad (3)$$

$$Z_\infty = \frac{K_0(s')}{2\pi k_{ep}Ls'K_1(s')} \quad (4)$$

where $s = (\phi_{Ni}/2)\sqrt{(p/\alpha_{Ni})}$ and $s' = (\phi_{Ni}/2)\sqrt{(p/\alpha_{ep})}$, p is the Laplace variable, I_0, K_0 and K_1 are Bessel functions, P_0 is the electrical power dissipated in the wire, k_{Ni} and k_{ep} are the thermal conductivities, α_{Ni} and α_{ep} are the thermal diffusivities, $\rho C_{p_{Ni}}$ and $\rho C_{p_{ep}}$ are the volumetric specific heats of respectively nickel (Ni) and epoxy resin (ep). The analytical average temperature T of the wire is then obtained from the temperature in Laplace domain $\theta(p,R_i)$ using the numerical inversion technique of Gaver–Stehfest:

$$T(t,R_i) = \frac{\ln(2)}{t}\sum_{j=1}^{20} V_j\theta\left(\frac{j\ln(2)}{t},R_i\right) \quad (5)$$

where the V_j coefficients can be found in [7].

4. Sensitivity analysis

All the calculations in this section were performed with a final temperature rise ΔT of only 2 K, via the adjustment of the electrical power P_0. This low temperature increase ensures variations of thermo-physical properties of materials with temperature lower than 1.5% and variations of the interfacial thermal resistance R_i lower than 5.7% as could be checked using final estimates.

The thermal model described by Eq. (5) allows to calculate, with respect to the thermo-physical parameters m, the reduced sensitivity coefficients X_m of the wire temperature given by

$$X_m = m\frac{\partial T}{\partial m} \quad \text{with } m = R_i,\ k_{ep},\ \rho_{ep}C_{p_{ep}},\ k_{Ni} \text{ or } \rho_{Ni}C_{p_{Ni}} \quad (6)$$

Fig. 3 shows that the sensitivity to R_i is quite low and that the maximum sensitivity values are obtained for the polymer thermal

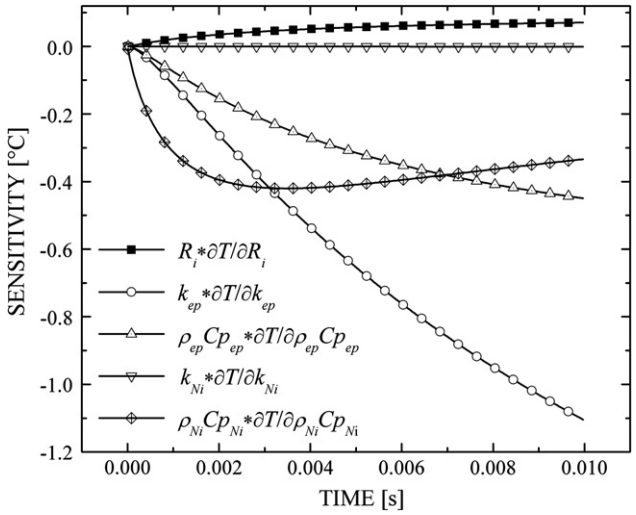

Fig. 3. Sensitivities of T to different parameters used in the thermal model ($\varphi_{Ni} = 26.9$ μm, $T = 20$ °C, $\Delta T = 2$ K, $\Delta t = 10$ ms, $R_i = 0.4\times10^{-5}$ m^2 K W^{-1}, $k_{ep} = 0.21$ W m^{-1} K^{-1}, $\rho_{ep}C_{p_{ep}} = 1.500\times10^6$ J m^{-3}, $k_{Ni} = 90.9$ W m^{-1} K^{-1}, $\rho_{Ni}C_{p_{Ni}} = 3.955\times10^6$ J m^{-3}).

conductivity k_{ep}. Considering that the sensitivity to the nickel thermal conductivity is very low and that it is easy to measure heat capacities with accuracy using DSC calorimeters, only R_i and k_{ep} were considered in the following as the parameters to be estimated.

Due to low sensitivity of the measurement to R_i, it was useful to find the values of experimental parameters (especially the heating time Δt) which optimize the estimation procedure (Fig. 4). The R_i and k_{ep} sensitivity coefficients were calculated for different heating times from 1 ms to 1 s while keeping the same final temperature rise $\Delta T = 2$ K (Fig. 4). It is interesting to note that the sensitivities strongly depend on the value of R_i, and that sensitivity to R_i is quite low compared to that of k_{ep}, especially for long heating times. It can also be seen that a low heating period reduces the preeminence of k_{ep}. For $R_i = 10^{-5}$ m^2 K W^{-1} (order of magnitude of the final experimental results), the maximum sensitivity to R_i appears for a heating period of 10 ms. This latter value was used during our experimental runs.

Note that in the estimation process, the parameters R_i and k_{ep} were found by minimizing the sum of the ordinary squared differences, cf. Eq. (7), between experimental (T_{exp}) and computed temperatures (T) of nickel wires using Eq. (5) and the SIMPLEX method [8], assuming all other parameters are known and have exact values.

$$J = \sum_{i=1}^{N}(T_{exp}-T)^2 \quad \text{with } \Delta t = N\,dt \quad (7)$$

The parameters obtained are average values along the length of the wire, as we've considered an average temperature of the nickel wire (1D heat transfers). If we had considered 2D heat transfers, we would have obtained a distribution of R_i along the wire related to the temperature profile. The assumption of 1D heat transfer is developed in Section 6, where it is shown that errors on parameters estimation due to axial heat losses are quite low.

5. Materials

Three cylindrical samples were made from three stretched nickel wires with diameters of 26.9, 55.8 and 122.9 μm and surrounded by a thermoset matrix. The polymer matrix provided by Huntsman [9] is an epoxy resin which is a mixture of 100 parts of

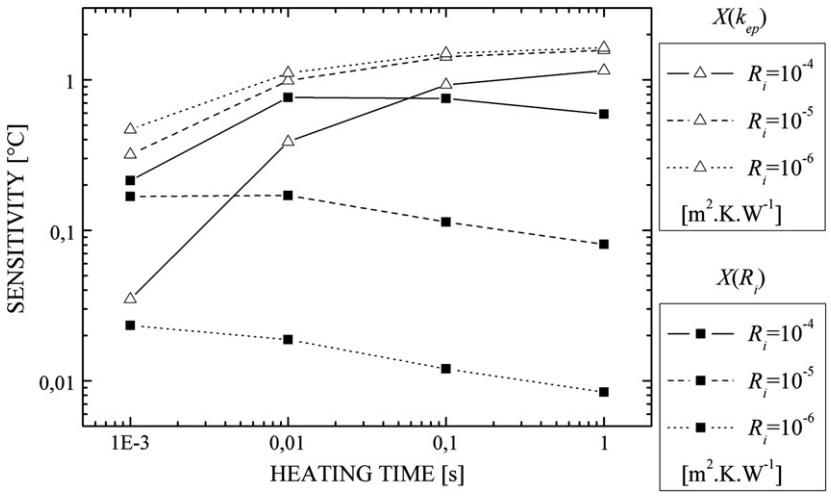

Fig. 4. Sensitivity coefficients of T with respect to R_i and k_{ep} at the end of the heating ($\phi_{Ni} = 26.9$ μm).

Araldite resin LY5052 and 38 parts of Aradur hardener HY 5052. Air bubbles after the mixing of the two resin components were removed using a vacuum pump. For the manufacturing of the samples, three cylindrical Teflon moulds were realized with Teflon plugs at their extremities. For each mould, two plugs were used with two copper wires of 1.6 mm diameter which went right through the plugs, and between which the nickel wires have been connected. A resin transfer moulding process at room temperature ($T = 20$ °C) and atmospheric pressure ($P = 10^5$ Pa) was used to fill the moulds.

6. Axial heat loss effect on R_i estimation

The most important source of bias in the hot-wire technique is usually the axial heat loss by conduction through the metallic wire. Due to the difficulties to mould the resin around small wires, we did not choose to eliminate end effects by using two wires different in length, or three wires method. We choose to use long wires and to compute the effect of heat losses on the estimated interfacial thermal resistances using a 2D finite element simulation. So, using a 2D axisymmetric geometry, see Fig. 5, with materials properties (k_{ep},…) and all internal and external boundary conditions (interfacial thermal resistance R_i between wire and matrix, initial temperature outside the polymer matrix, and initial temperature at the axial extremities of the sample which creates 2D heat transfer), the temperature of the nickel wire was computed and averaged along its axis since it was not uniform. Then using this temperature evolution during a heating in the estimation procedure (based on the 1D thermal model, Eq. (5)), an interfacial resistance R_i^{2D} and a polymer thermal conductivity k_{ep}^{2D} were estimated, see Fig. 6. Table 1 shows the relative discrepancies $\Delta R_i/R_i$ and $\Delta k_{ep}/k_{ep}$ between initially considered and estimated parameters which are modified because of the wire end effects. The values of $\Delta R_i/R_i$ and $\Delta k_{ep}/k_{ep}$ were computed using Eq. (8):

$$\frac{\Delta R_i}{R_i} = \frac{R_i - R_i^{2D}}{R_i} \quad \text{and} \quad \frac{\Delta k_{ep}}{k_{ep}} = \frac{k_{ep} - k_{ep}^{2D}}{k_{ep}} \tag{8}$$

It can be seen in Table 1 that the biases due to end effects are quite low. They are lower than 3% for k_{ep} which is close to accuracy of ordinary measurement methods and 7% for R_i which is quite low compared to errors on R_i which are usually about 20%. These biases are overestimated since a prescribed temperature equal to the initial temperature at the sample and wire ends was considered in the 2D heat transfer model, resulting in increased biases. Indeed, in our samples the nickel wires are welded to copper wires, so considering a prescribed temperature equal to the external one at the ends provides much higher bias.

7. Reproducibility analysis – uncertainties on the estimated parameters

To test the reproducibility of the R_i measurement, five runs were systematically performed for each initial uniform temperature and each sample with different wire diameters. Table 2 reports the results of the five repeated runs for the sample with a nickel wire diameter of 26.9 μm and for an initial temperature of 20 °C. The R_i values are very similar, the discrepancies do not exceed 5.2%. It is also true for the estimated conductivity of the epoxy resin (0.21 W m^{-1} K^{-1}) which, in addition, is very close to the value provided by the guarded hot plate method (0.22 W m^{-1} K^{-1}).

The root mean square values, δ_{RMS}, of the temperature residuals are very low due to very accurate temperature and known parameters' measurements. However, the δ_{RMS} values are about 0.01 °C and are only seven times smaller than the reduced sensitivity coefficient that we have computed for $R_i = 0.4 \times 10^{-5}$ m^2 K W^{-1} with a heating time Δt of 10 ms (Fig. 3). It would have been difficult to perform parameter estimation with much smaller R_i values because δ_{RMS} would have been too close to the sensitivity coefficients of temperature with respect to R_i. This shows the difficulties of performing R_i measurements.

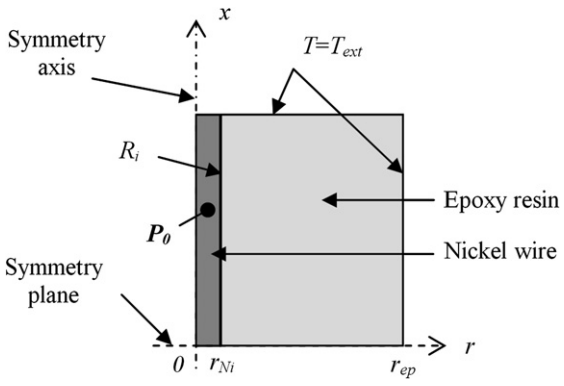

Fig. 5. 2D axisymmetric geometry used to study heat loss effects.

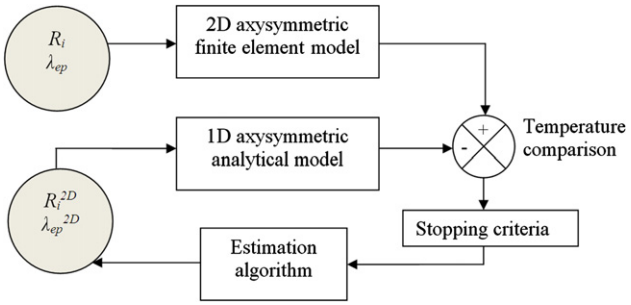

Fig. 6. Procedure used to estimate bias on R_i estimation due to axial heat loss.

In Table 2, absolute uncertainties $2\sigma_{R_i}$ and $2\sigma_{k_{ep}}$ on the estimated parameters R_i and λ_{ep} with confidence intervals of 95% comes from the calculation of the matrix of variance–covariance S^{final} at the final iteration as proposed by Milosevic [10] and defined by Eq. (9):

$$S^{final} = \left[X^T \quad W \quad X\right]^{-1} \tag{9}$$

$$\text{with } (W)_{nn} = \left[\sigma_T^2 + \sum_k \left(\sigma_{m_k}\frac{\partial T_n}{\partial m_k}\right)^2\right]^{-1} \text{ and } (X)_{nm} = \frac{\partial T_n}{\partial m}, \quad m = R_i \text{ or } k_{ep} \tag{10}$$

where the standard deviation σ_T is calculated from the temperature residuals and is related to the noise on temperature measurements. The standard deviations σ_{m_k} are associated with errors on the known parameters which were evaluated from their relative values: $\varepsilon_{P_0} = 0.4\%$, $\varepsilon_{\phi_{Ni}} = 0.2\%$, $\varepsilon_{\rho_{Ni}C_{p_{Ni}}} = 1\%$, $\varepsilon_{\rho_{ep}C_{pep}} = 1\%$ and $\varepsilon_{k_{Ni}} = 3\%$. The uncertainties σ_{R_i} and $\sigma_{k_{ep}}$ on the estimated parameters R_i and k_{ep} are then deduced from the diagonal terms of the matrix S^{final}, which are the variances related to R_i and k_{ep}.

8. Effect of temperature and wire diameter

A set of 45 runs was performed for three different initial temperatures (20, 35 and 50 °C) and for three nickel wire diameters ϕ_{Ni} (26.9, 55.8 and 122.9 μm), each measurement being repeated five times. The Wheatstone bridge unbalanced and supply voltages were recorded versus time using two differential probes (Tektronix ADA400A) and a numerical oscilloscope (Tektronix TDS 5052). Fig. 7 shows the measured temperature and electrical power during one run. Residuals between experimental and calculated temperatures have also been plotted, see Fig. 8, and it can be seen that they are small and well scattered around zero. The results of the interfacial thermal resistance estimation are presented in Table 3, each value being the average of five runs. It appears that R_i increases with both temperature and wire diameter. When the temperature rises from 20 to 50 °C, R_i values are multiplied by a factor of 1.4, 1.6 and 1.9 for wire diameters of respectively 26.9, 55.8 and 122.9 μm. Therefore, the higher the wire diameter is, the more the R_i values increase with initial temperature. Within the studied temperature and wire diameter ranges, the R_i dependencies are linear as shown in Figs. 9 and 10.

Table 1
Bias on R_i estimation due to axial heat loss at the end of the nickel wires.

ϕ_{Ni} (μm)		26.9	55.8	122.9
$\Delta R_i/R_i$ (%)	$R_i = 0.5\times10^{-5}$ (m² K W⁻¹)	3.6	6.5	4.8
	$R_i = 5\times10^{-5}$ (m² K W⁻¹)	4.2	5.3	3.8
$\Delta k_{ep}/k_{ep}$ (%)	$R_i = 0.5\times10^{-5}$ (m² K W⁻¹)	2.7	2.7	2.1
	$R_i = 5\times10^{-5}$ (m² K W⁻¹)	2.2	1.7	1.5

Table 2
Reproducibility tests for the sample with the 26.9 μm nickel wire in epoxy resin ($T = 20$ °C, $\Delta t = 10$ ms).

Run no.	ΔT (K)	k_{ep} (W m⁻¹ K⁻¹)	R_i (10^{-5} m² K W⁻¹)	δ_{RMS} (°C)
1	2.09	0.21 ± 0.005	0.40 ± 0.10	0.009
2	2.09	0.21 ± 0.005	0.39 ± 0.10	0.011
3	2.07	0.21 ± 0.005	0.37 ± 0.10	0.009
4	2.11	0.21 ± 0.005	0.37 ± 0.10	0.01
5	2.08	0.21 ± 0.005	0.37 ± 0.10	0.011

9. Thermo-elastic analysis

The samples were manufactured at ambient temperature and pressure (i.e. $T = 20$ °C, and $P = 10^5$ Pa), therefore the temperature increase should result in a gap at the polymer/metallic wire interface because the thermal expansion coefficient for epoxy is much higher than that of nickel as shown in Table 4. We have tried to compare the thermal resistance of this unsticking area with our previously measured interfacial thermal resistance.

Assuming a zero contact pressure at the interface at the manufacturing temperature of 20 °C, the theory of thermo-elasticity, [11, §151 – Eq. (h)], allows to calculate the displacements u_j at the interface of the two concentric cylindrical mediums considered as isothermal and initially in contact:

$$u_j = (1+\nu_j)\beta_j\frac{\phi_{Ni}}{2}T_i, \quad j = \text{Ni or ep} \tag{11}$$

where β_j is the thermal expansion coefficient and ν_j the Poisson's ratio (Table 4) and T_i the temperature. The gap thicknesses, (u_{ep}–u_{Ni}), calculated with Eq. (11) are shown in Table 5. The values are between 20 nm and 209 nm. As the mean free path of air molecule is about 68 nm (Knudsen number between 0.3 and 3), we can use the thermal conductivity law for confined air developed for porous medium [12]:

$$k_g = \frac{k_g^0}{1 + \left(k_g^0/Pe\right)\sqrt{(\pi\overline{M}T_i/2\overline{R})}} \tag{12}$$

where k_g^0 is the thermal conductivity of the free air, P the pressure, e the thickness of the confined cavity, M the air molar mass and R the ideal gas constant.

Then, the thermal resistance of the air gap can be calculated using

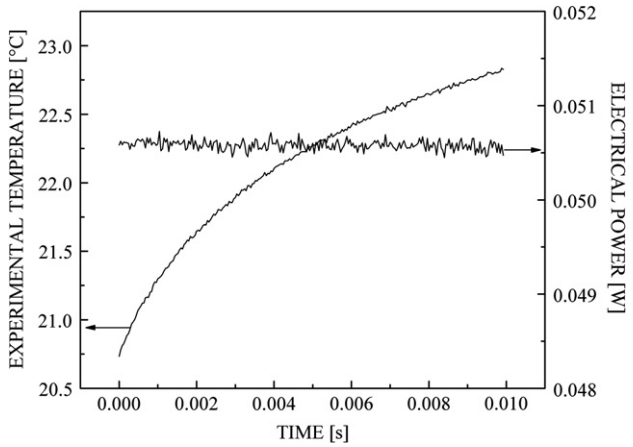

Fig. 7. Experimental temperature and electrical power versus time ($T_i = 20$ °C, $\phi_{Ni} = 26.9$ μm).

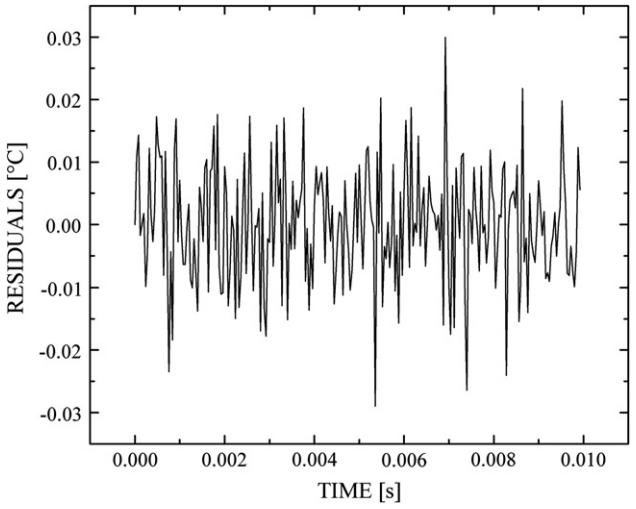

Fig. 8. Temperature residuals ($T_i = 20\ °C$, $\phi_{Ni} = 26.9\ \mu m$).

$$R_{air} = \frac{u_{ep} - u_{Ni}}{\lambda_{air}} \tag{13}$$

Table 6 presents the calculated air gap thermal resistance only for gap thicknesses larger than the mean free path of air molecule to insure the validity of Eq. (12). It can be seen that the calculated thermal resistances are a little bit higher than the measured interfacial thermal resistance. Discrepancies could come from the assumptions that were used to calculate the gap thermal resistances. The interstitial gas could be different from air due to gas release from the polymer. In addition, at the manufacturing temperature of 20 °C, no contact pressure was considered. There should exist some contact pressure because of the chemical shrinkage of epoxy (about 3–4%) during sample manufacturing. This study is in fact well-adapted to compare orders of magnitude between thermal interface resistance and air gap thermal resistance, but does not allow to calculate precise values for thermal resistances.

10. Conclusion

Interfacial thermal resistances have been measured between epoxy resin and thin nickel wires tight in the mould before the epoxy transfer. The heating of the wire was provided by Joule effect and its temperature was obtained through the recording of its electrical resistance. The wire/matrix interface resistance has been estimated using a thermal model developed using the quadrupoles method. A sensitivity analysis was performed to choose the heating time (typically 10 ms) in order to reduce uncertainties on the estimated parameters. Tests were performed for different nickel wire diameters (26.9, 55.8 and 122.9 μm) and different temperatures (20, 35 and 50 °C). The measured interfacial thermal resistances for nickel wire and epoxy resin are between 0.4×10^{-5} and $1.6 \times 10^{-5}\ m^2\,K\,W^{-1}$. The thermal interface resistance increases

Table 3
Estimated interfacial thermal resistances R_i ($10^{-5}\ m^2\,K\,W^{-1}$).

T (°C)	ϕ_{Ni} (μm)		
	26.9	55.8	122.9
20	0.38 ± 0.10	0.57 ± 0.13	0.87 ± 0.13
35	0.48 ± 0.07	0.69 ± 0.09	1.27 ± 0.13
50	0.53 ± 0.08	0.90 ± 0.12	1.63 ± 0.12

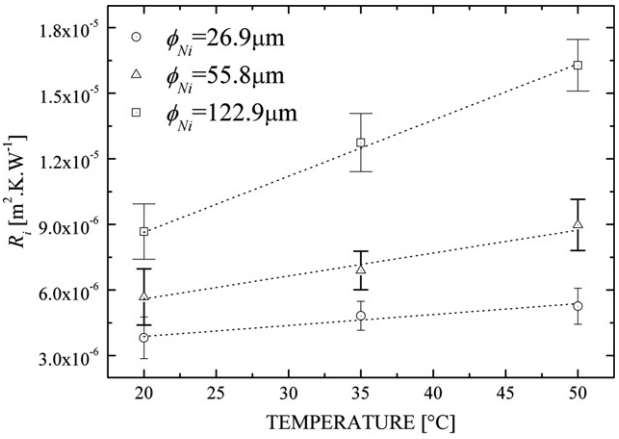

Fig. 9. Effect of temperature on the interfacial thermal resistance R_i.

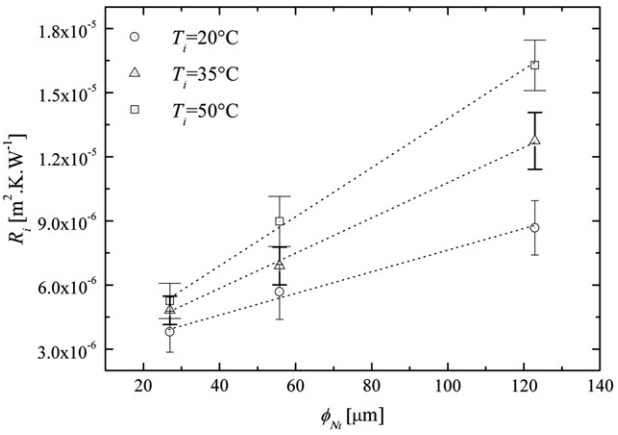

Fig. 10. Effect of nickel wire diameter on the interfacial thermal resistance R_i.

Table 4
Poisson's ratio (ν) and thermal expansion coefficient (β) for nickel and epoxy resin.

	Nickel	Epoxy
ν	0.312	0.35
β ($10^{-6}\ K^{-1}$)	13.3	97

Table 5
Gap u_{ep}–u_{Ni} (μm) versus temperature and nickel wire diameter.

T_i (°C)	ϕ_{Ni} (μm)		
	26.9	55.8	122.9
20	0	0	0
35	0.023	0.047	0.104
50	0.046	0.095	0.209

Table 6
Thermal resistance of the air gap ($10^{-5}\ m^2\,K\,W^{-1}$) and the measured interfacial thermal resistance ($10^{-5}\ m^2\,K\,W^{-1}$).

T_i (°C)	ϕ_{Ni} (μm)		
	26.9	55.8	122.9
20	–	–	–
35	–	–	1.68 (1.27)
50	–	1.64 (0.90)	2.1 (1.63)

sharply with the temperature with a factor between 2 and 3 for a temperature increase of only 30 K. In addition, the interfacial thermal resistance varies with the wire diameter, which shows – in our case – the non-validity of the assumption used in the usual effective thermal conductivity models that R_i is constant whatever the size of particles.

References

[1] C. Filip, B. Garnier, F. Danes, Effective conductivity of a composite in a primitive tetragonal lattice of highly conducting spheres in resistive thermal contact with the isolating matrix, J. Heat Transfer 129 (12) (2007) 1617–1626.

[2] D.P.H. Hasselman, K.Y. Donaldson, Effective thermal conductivity of uniaxial composite with cylindrically orthotropic carbon fibers and interfacial thermal barrier, J. Compos. Mater. 27 (6) (1993) 637–644.

[3] F. Macedo, J.A. Ferreira, Thermal contact resistance evaluation in polymer-based carbon fiber composites, Rev. Sci. Inst. 74 (1) (2003) 828–830.

[4] B. Garnier, T. Dupuis, J. Gilles, J.-P. Bardon, F. Danès, Thermal contact resistance between matrix and particle in composite materials measured by a thermal microscopic method using a semi-intrinsic thermocouple, In: 12th Int. Heat Transfer Conf., 2002, pp. 9–14.

[5] M.J. Assael, K.D. Antoniadis, D. Tzetzis, The use of the transient hot-wire technique for measurement of the thermal conductivity of an epoxy-resin reinforced with glass fibres and/or carbon multi-walled nanotubes, Compos. Sci. Technol. 68 (15–16) (2008) 3178–3183.

[6] H. Xie, H. Gu, M. Fujii, X. Zhang, Short hot wire technique for measuring thermal conductivity and thermal diffusivity of various materials, Measure. Sci. Technol. 17 (1) (2006) 208–214.

[7] D. Maillet, S. Andre, J.-C. Batsale, A. Degiovanni, C. Moyne, Thermal Quadrupoles, Wiley, Chichester, 2000.

[8] J.C. Lagarias, J.A. Reeds, M.H. Wright, P.E. Wright, Convergence properties of the Nelder–Mead simplex method in low dimensions, SIAM J. Optim. 9 (1) (1998) 112–147 Society for Industrial and Applied Mathematics.

[9] Huntsman Llc, Advanced Materials (Structural Composites), Cold-curing epoxy system based on Araldite LY 5052/Aradur 5052 (Data Sheet), March 2004.

[10] N.D. Miloševic, M. Raynaud, K.D. Maglic, Estimation of contact resistance between the materials of double-layer sample using the laser flash method, Inverse Prob. Eng. 10 (1) (2002) 85–103.

[11] S.P. Timoshenko, J.N. Goodier, Theory of Elasticity, third ed. McGraw-Hill, New York, 1970.

[12] J. Gilles, J.-M. Goyheneche, F. Enguehard, Modelisation du transfert thermique dans un isolant microporeux, Congrès français de Thermique (2000) (SFT, Lyon), Elsevier511–516.